iScience, Volume *26*

Supplemental information

Transcriptional and metabolic programs promote the expansion of follicular helper T cells in lupus-prone mice

Minghao Gong, Seung-Chul Choi, Yuk Pheel Park, Xueyang Zou, Ahmed S. Elshikha, Valerie A. Gerriets, Jeffrey C. Rathmell, Mansour Mohamazadeh, and Laurence Morel

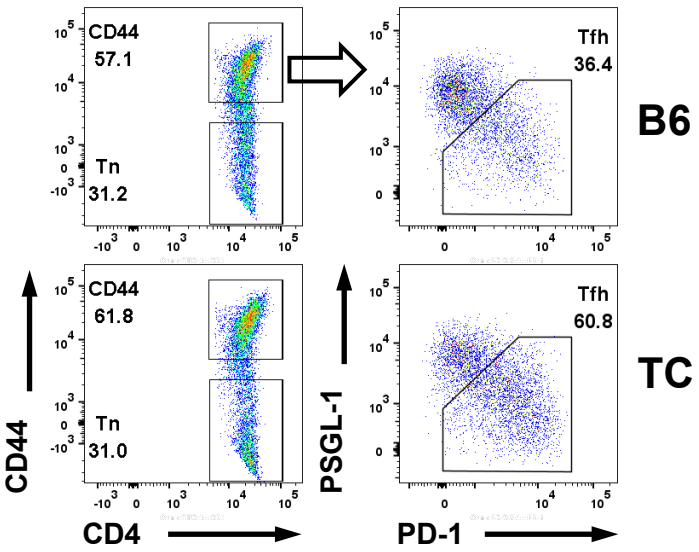

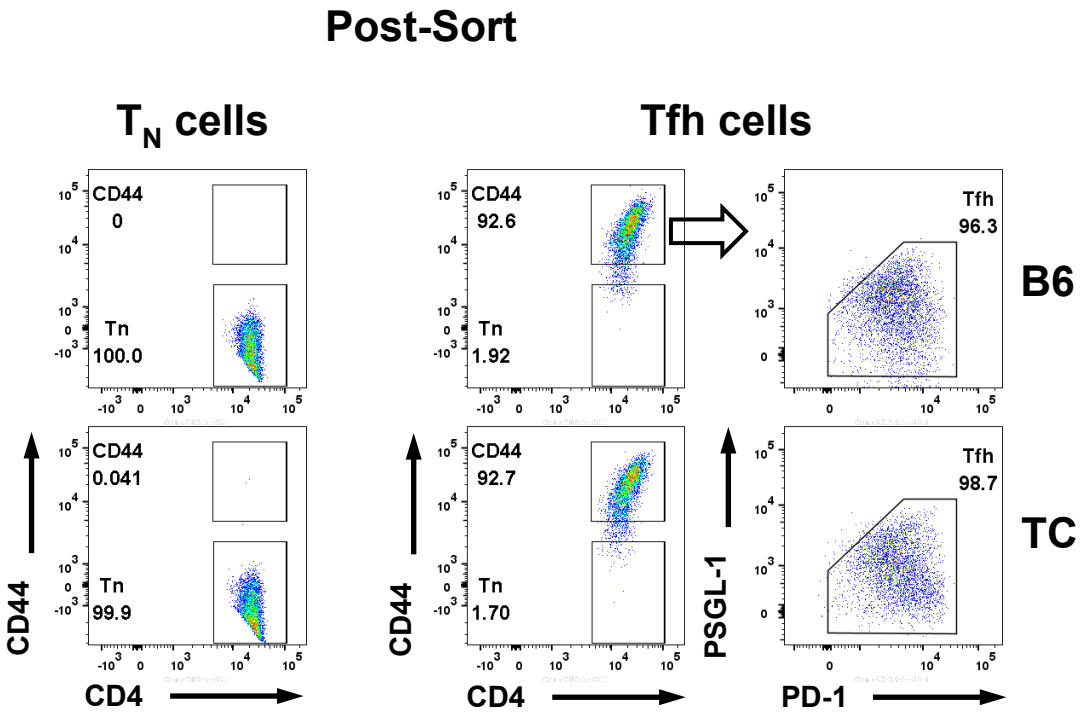

Figure S1, related to Figure 1. Gating strategy and purity of sorted Tfh and Tn cells from TC and B6 mice. The representative FACS plots show CD4, CD44, PD-1 and PSGL-1 staining in purified splenic CD4+ T cells pre- (top) and post (bottom) sort. The percentages of CD44- TN and CD44+PSGL-1lo PD-1+ TFH cells are indicated for each gate.

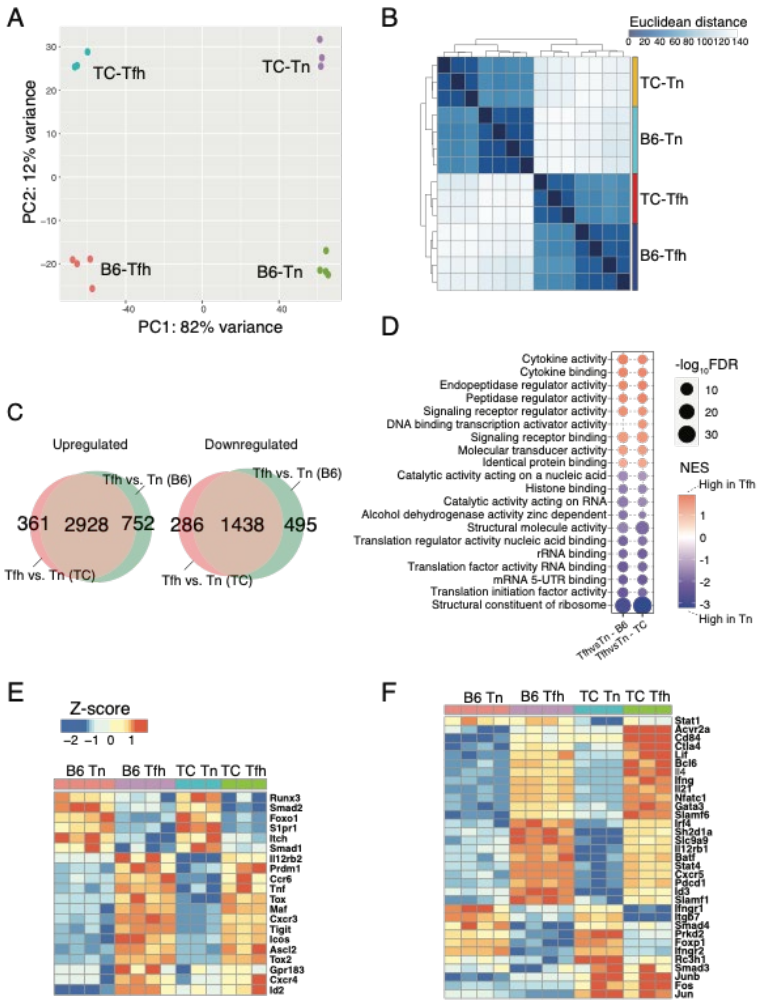

Figure S2. TC and B6 mice share a majority of transcriptional projections from Tn to Tfh cells, related to Figure 1. RNA-seq data of Tfh and Tn cells isolated from TC (n = 3) and B6 (n = 4) mice.

(A) Principal component analysis.

(B) Hierarchical clustering analyses of the Euclidian distance matrix of the indicated groups.

(C) Venn diagrams visualizing DEGs comparing Tfh to Tn cells shared between the TC and B6 strains. The non-shared DEGs were uniquely down- (right) or up- (left) regulated in TC (pink) or B6 (green) Tfh cells.

(D) Bubble plot of top 20 Tfh vs. Tn GSEA sets in TC and B6 mice filtered by FDR-corrected $p < 0.05$. The color scale indicates NES and the size of the symbols indicates levels of significance. The inputs were ranked gene lists based on Wald-statistic scores comparing Tfh vs. Tn in either TC or B6 mice. The gene sets were obtained from the Gene Ontology Molecular Function database.

(E-F) Heatmaps showing Z-scores transformed from regularized-log2-converted counts of Tfh-signature genes in Tfh and Tn cells from B6 and TC mice. Tfh-signature genes with expression levels that are not significantly different (E) or significantly different (F) in TC compared to B6 Tfh cells.

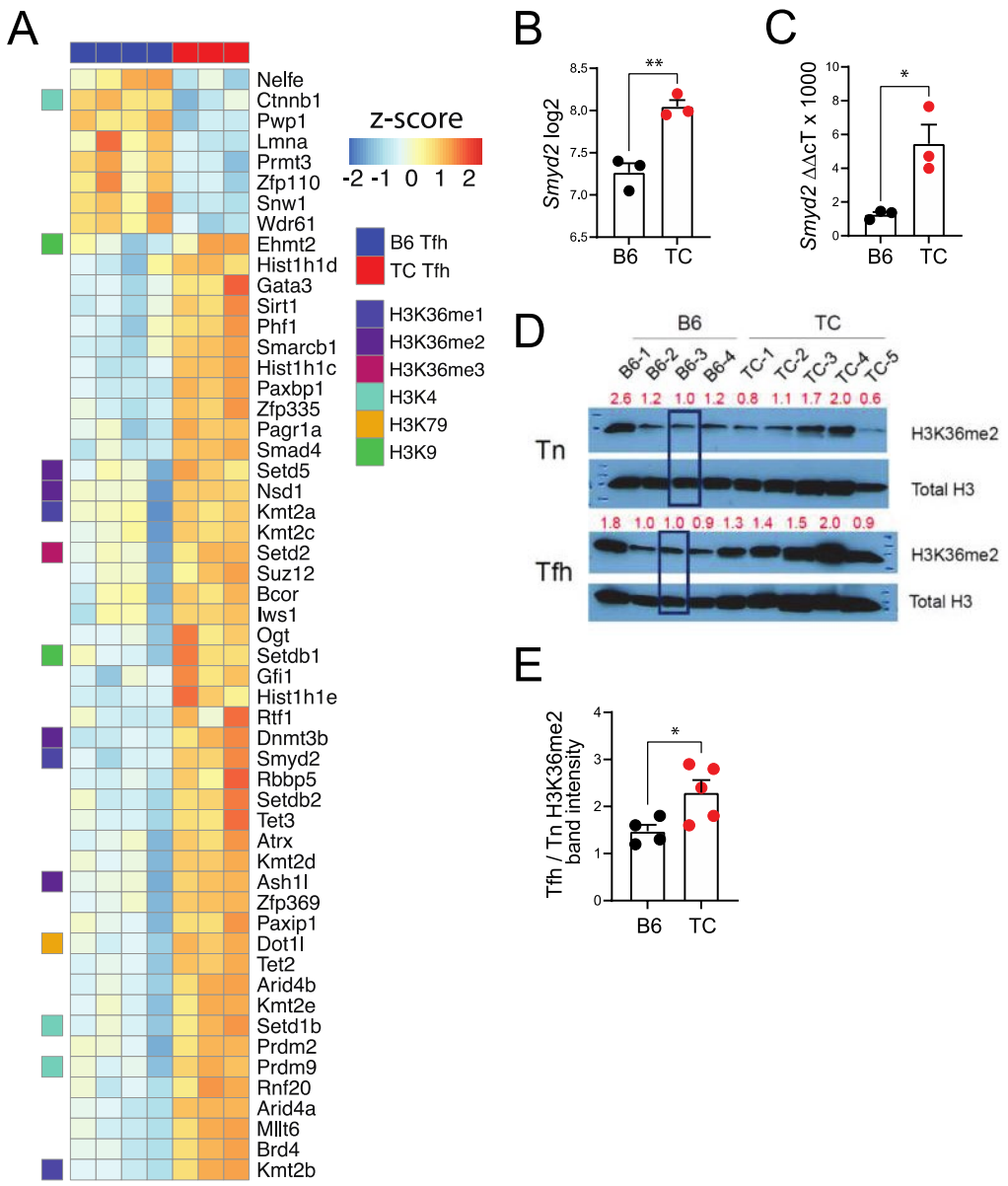

Figure S3. TC Tfh cells express a chromatin-modification signature, related to Figure 2.

(A) Heatmap showing Z-scores transformed from regularized-log2-converted counts of DEGs in the histone methylation pathway (FDR-corrected $p < 0.05$, Wald test). The histone H3 lysine methylation function indicated in the legend is indicated for the corresponding genes in the track on the left.

(B) Tfh expression of *Smyd2* in the RNASeq dataset.

(C) Tfh expression of *Smyd2* assessed by qRT-PCR.

(D) H3K36me2 levels assessed by Western blot in Tn and Tfh cells from B6 and TC mice (n = 4). The band intensities shown in red were expressed relative to total H3 amount and normalized to the boxed B6 samples as 1.

(E) Tfh/Tn H3K36me2 levels from the values shown in (D).

Each symbol in the graphs represents a mouse from a different cohort in B, C, and E. Mean and s.e.m. compared with 2-tailed *t* tests. *p<0.05, **p<0.01.

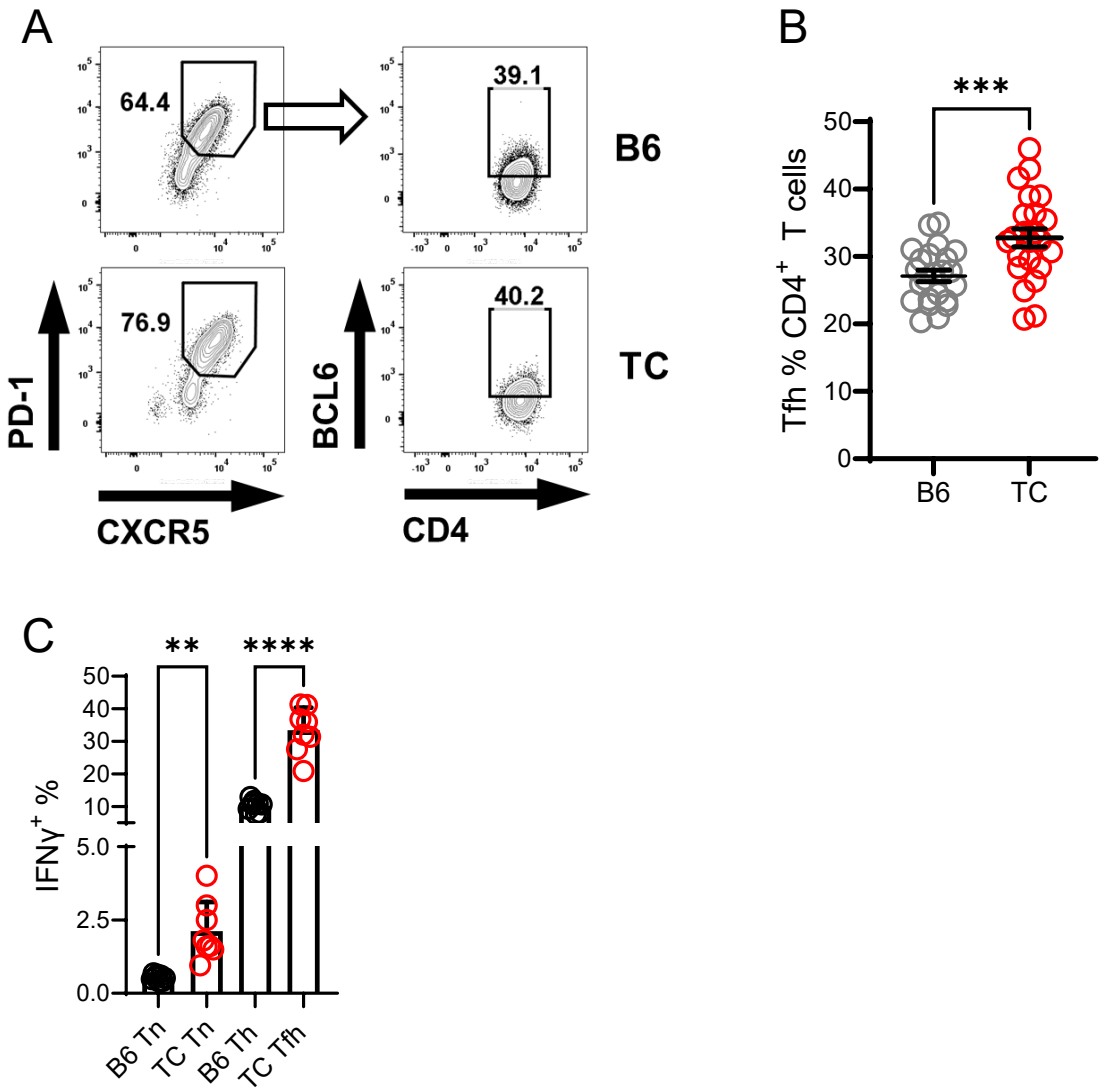

Figure S4, related to Figure 3. TC Tn cells show a greater response to Tfh polarization than B6 Tn cells.
(A) Representative FACS plots show *in vitro* differentiation of Tfh cells, gated as $CD4^+$ $CXCR5^+$ $PD\text{-}1^+$ $BCL6^+$, from B6 and TC Tn cells.
(B) Quantitation of Tfh cell frequency. Each symbol represents a mouse (n = 23) pooled from 6 experiments. Mean and s.e.m. compared with a 2-tailed *t* test. ***p<0.001. Related to Figure 2.
(C) *Ex-vivo* IFNγ expression by Tn and Tfh from B6 and TC mice. Each symbol represents a mouse (n = 8). Mean and s.e.m. compared with a Brown-Forsythe ANOVA with Dunnett's T3 multiple comparisons tests. **p<0.01, ****p<0.0001.

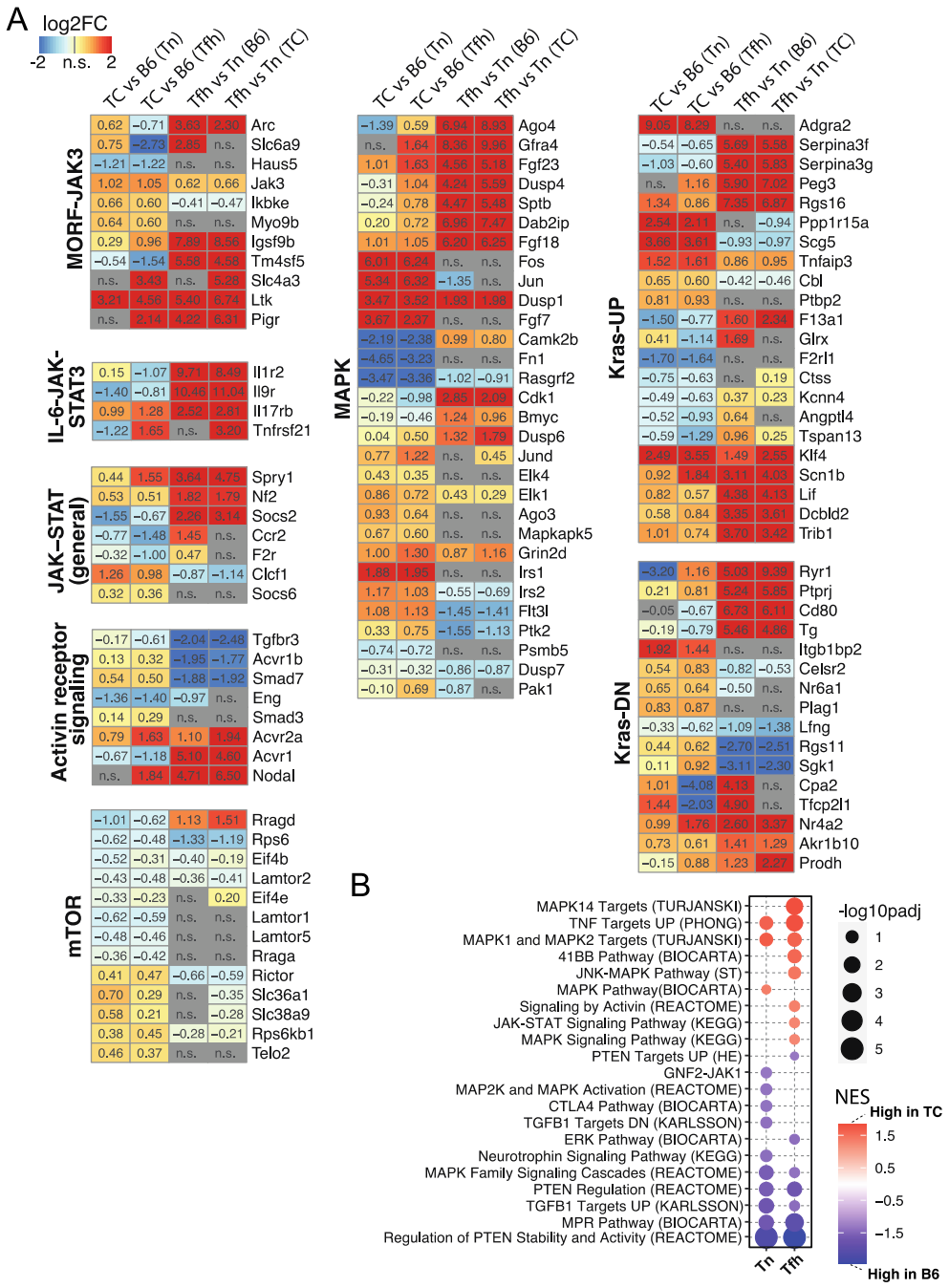

Figure S5. Altered expression of Tfh-signature genes and pathways in TC Tfh cells, related to Figure 3.

(A) Heatmaps for log2FC of DEGs (FDR-corrected p < 0.05) in each indicated comparison according to the color scale shown on the upper left. Genes were grouped by functional pathways indicated on the left of each cluster.

(B) Bubble plots of top significant gene sets related to cell signaling pathways. The inputs are derived from ranked gene lists (Wald-statistic scores) shown in (A) comparing separately Tn and Tfh cells between TC and B6 mice. Significant gene sets were filtered by FDR-corrected p < 0.05. The origin of gene sets is indicated in parentheses.

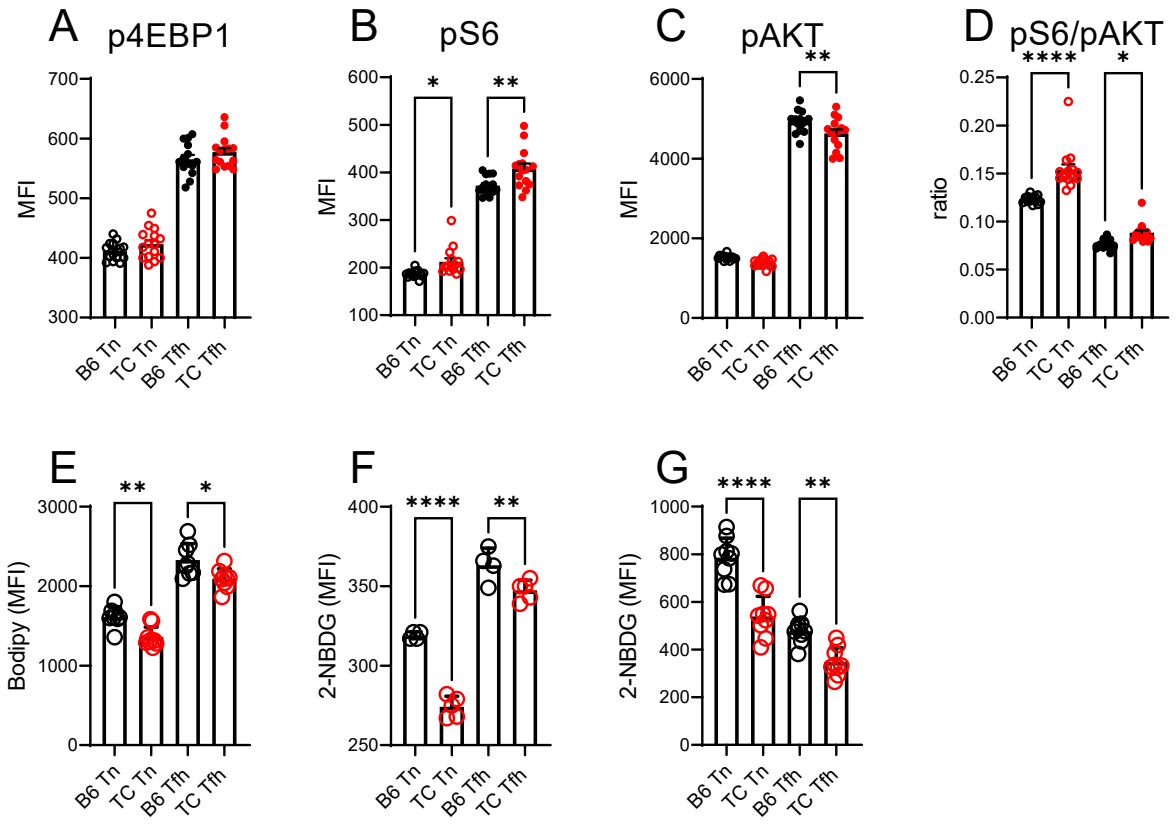

Figure S6. Metabolic alterations in Tn and Tfh TC cells, related to Figure 3.
(A – D) Expression of mTOR targets p4EBP1 (A), pS6 (B) and pS473ATK (C) in B6 and TC Tn and Tfh cells. (D) pS6 / pS473AKT ratio.
(E) Bodipy stain *in vitro*.
(F -G) Glucose (2NBDG) uptake *in vitro* (F) and *in vivo* (G).
Each symbol represents a mouse. A - D: n = 14 pooled from 4 cohorts, E - G: n = 4 - 10 pooled from 2 experiments. Means ± s.e.m analyzed by 1-way ANOVA with Dunnett's T3 multiple comparisons tests. *p<0.05, **p<0.01, ****p<0.0001.

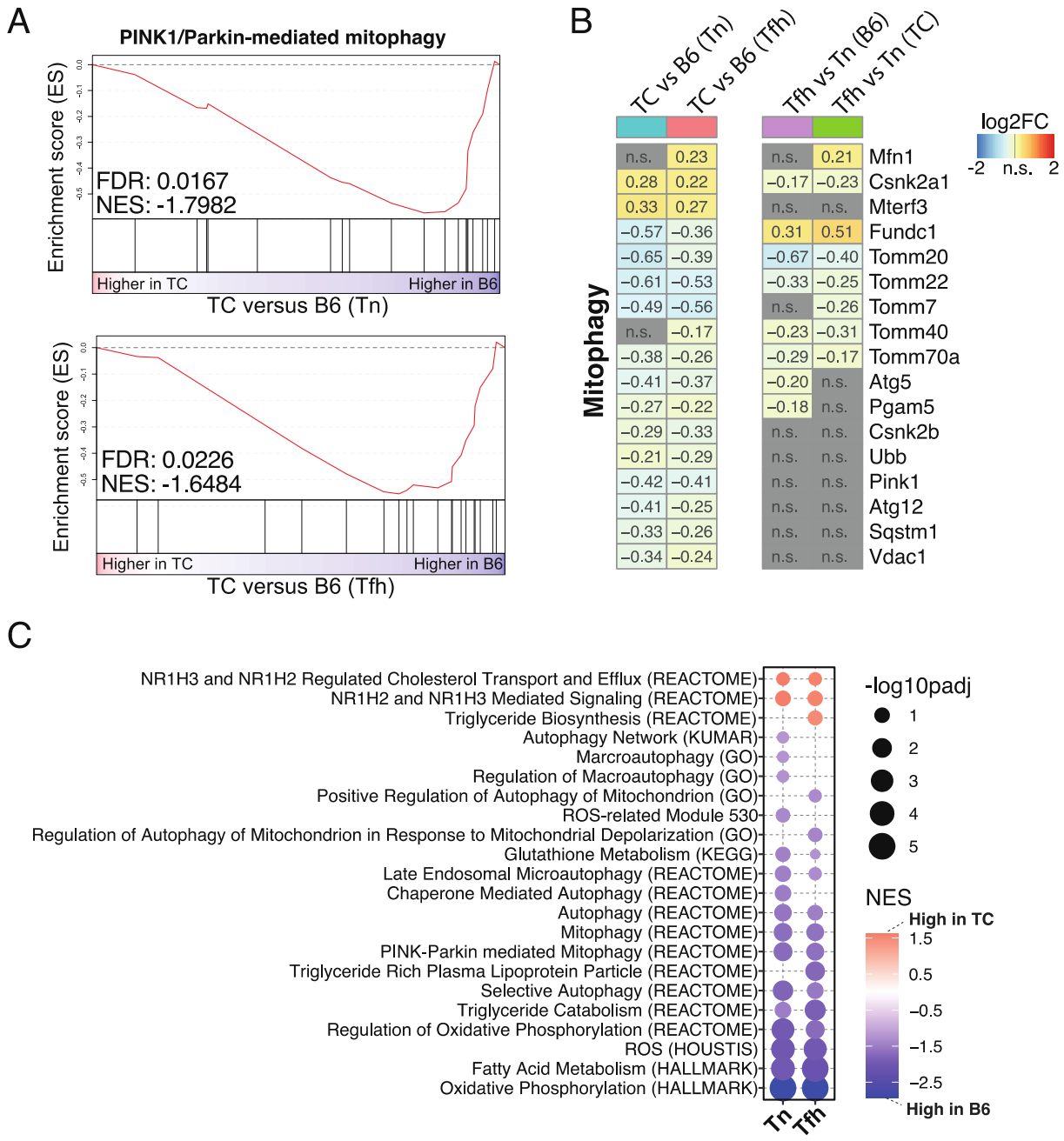

Figure S7. Defective mitophagy in TC Tn and Tfh cells, related to Figures 4 and 5.
(A) GSEA plots of the Pink/Parkin-mediated mitophagy gene set comparing TC and B6 Tn cells (top) and Tfh cells (bottom).
(B) Heatmap of log2FC for DEGs (FDR-corrected $p < 0.05$) of the data shown in (A).
(C) Bubble plot of top significant gene sets related to mitochondrial function. The inputs are ranked gene lists comparing separately Tn and Tfh cells between TC and B6 mice. Significant gene sets were filtered by FDR-corrected $p < 0.05$. The origin of the gene sets is indicated in parentheses.

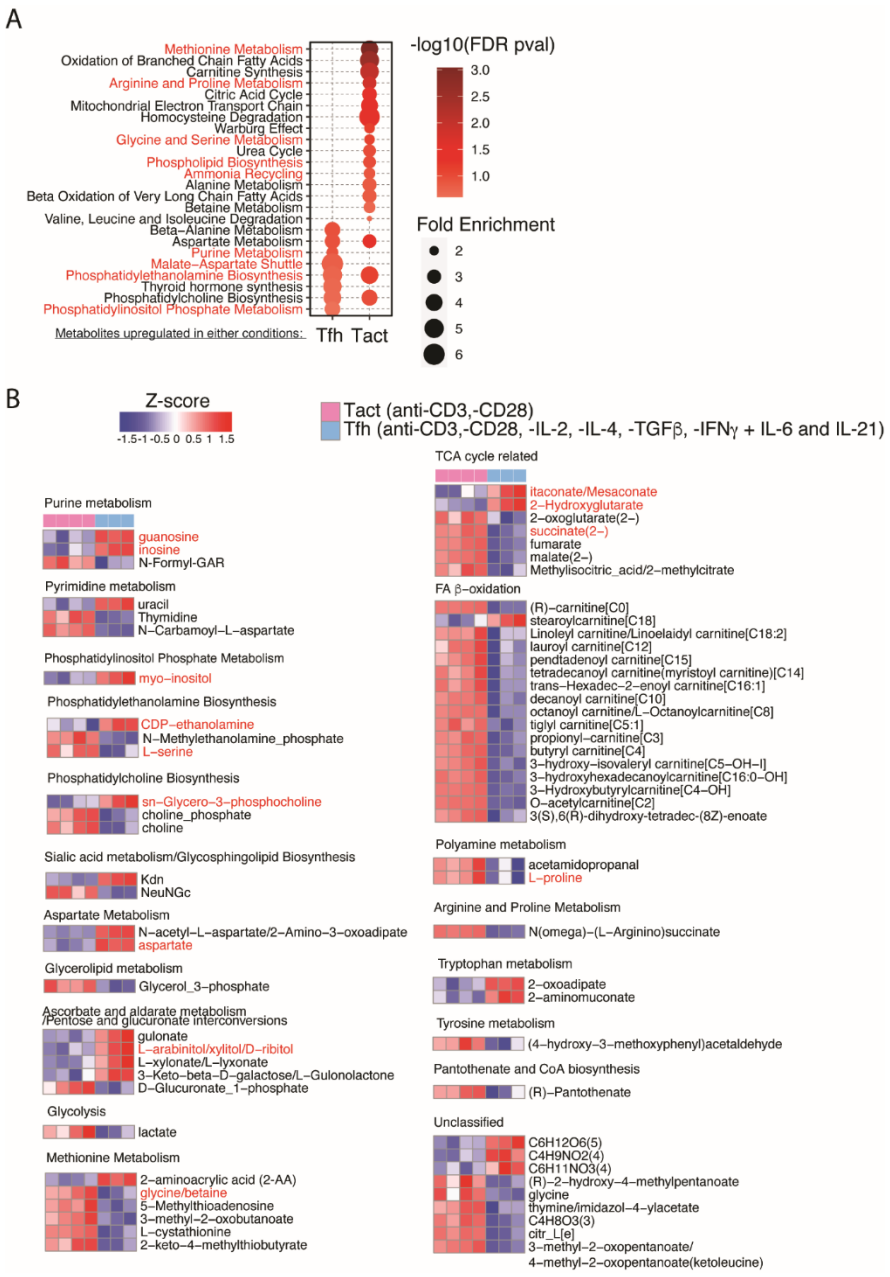

Figure S8. Metabolic phenotypes in polarized Tfh compared to non-polarized activated T (Tact) cells from B6 mice, related to Figure 6.

(A) Pathway analyses showing distinct metabolic pathways uniquely upregulated in Tfh cells (e.g., inositol phosphate metabolism, malate-aspartate shuttle) and downregulated in Tfh cells (e.g., mitochondrial metabolism and fatty acid β-oxidation). Significant pathways that are also metabolic signatures of TC Tfh cells are shown in red font (See Figure 6B). The inputs for pathway analysis are metabolites that were significantly upregulated in either Tfh cells (left) or Tact (right). Thus, the metabolic pathways (e.g., phosphatidylethanolamine biosynthesis) that are significant in both groups suggest the pathways are activated, though the direction is uncertain and should be further diagnosed by examining the dynamics between precursor and product metabolites showed in B. (B) Heatmaps display significantly enriched metabolites comparing Tfh to Tact cells, grouped by function.

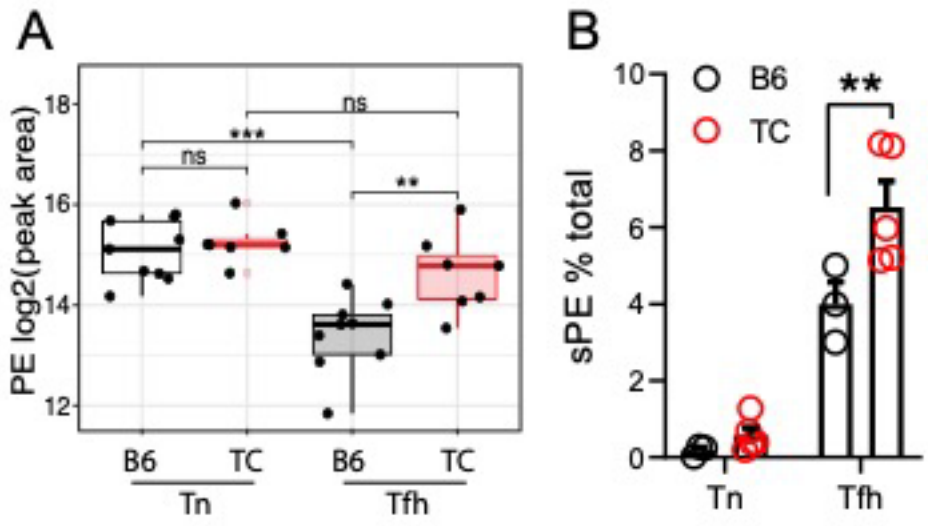

Figure S9. Phosphoethanolamine (PE) in B6 and TC Tn and Tfh cells, related to Figure 6.
(A) PE content detected by GC-TOF-MS, n = 7 - 9.
(B) Surface PE (sPE) relative to total (surface + intracellular) PE determined by flow cytometry, n = 3 B6 and 5 TC mice.
Each symbol represents a mouse. Means ± s.e.m analyzed by 1-way ANOVA with Dunnett's T3 multiple comparisons tests. **p<0.01, ***p<0.001.

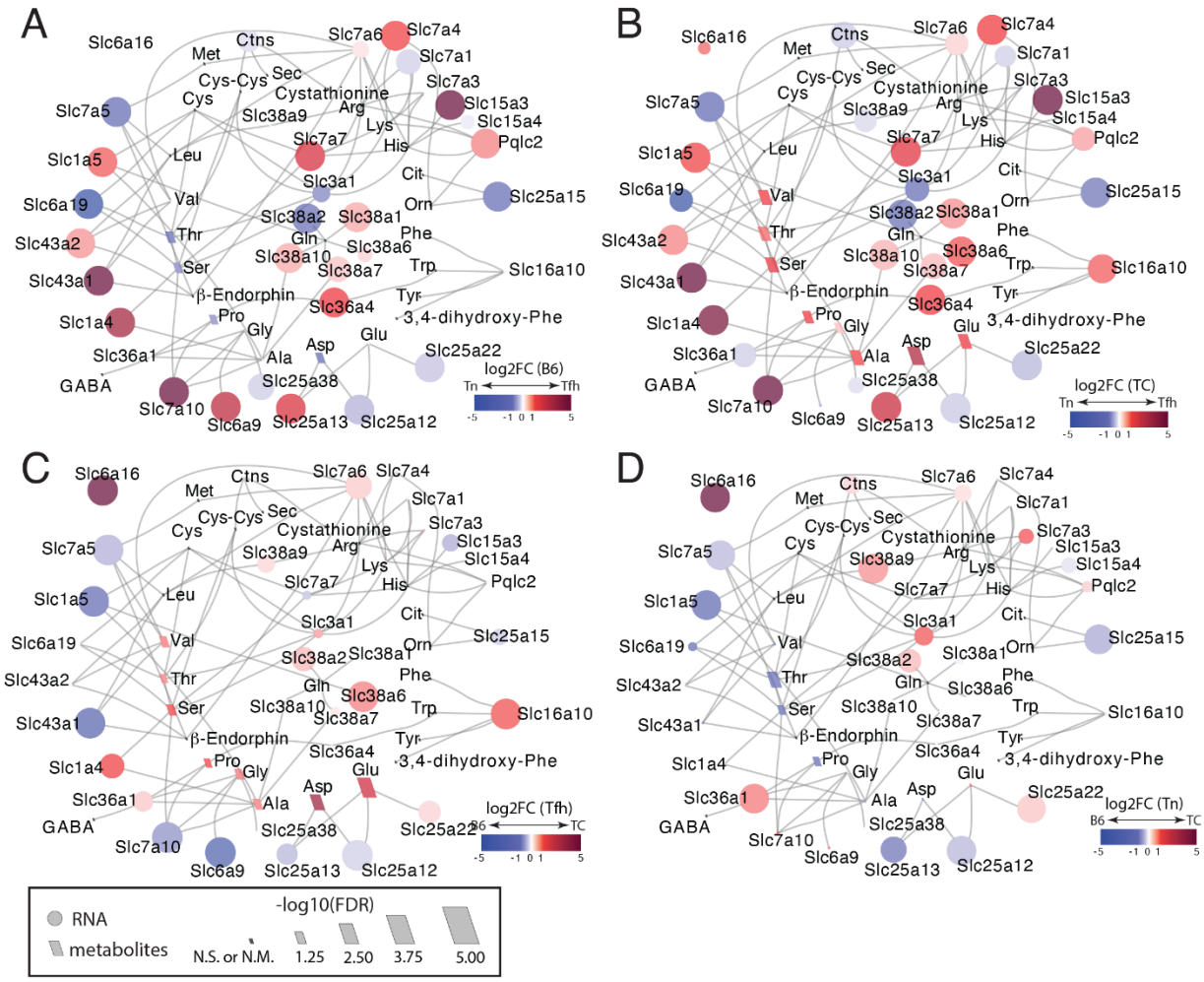

Figure S10. Increased amino acid trafficking in TC Tfh cells, related to Figure 6.

Network analysis of the dynamics of amino acids and their transporters combining RNA-seq and metabolomic results. The analyses include comparisons between Tfh and Tn cells of B6 origin (A) or of TC origin (B) and comparisons between TC and B6 in Tfh cells (C) or Tn cells (D). The size of the bubbles (transporter) or diamonds (amino acids) indicates the log10-transformed FDR-corrected p values. The color scale indicates magnitude of log2FC (log2FC > 5 is normalized to 5). The metabolomic data present here is based on one of the two cohorts.